

Irregular Repetition Slotted Aloha with Multiuser Detection: A Density Evolution Analysis

Manuel Fernández-Veiga, M.E. Sousa-Vieira, Ana Fernández-Vilas, Rebeca P. Díaz-Redondo

Abstract

Irregular repetition slotted Aloha (IRSA) has shown significant advantages as a modern technique for uncoordinated random access with massive number of users due to its capability of achieving theoretically a throughput of 1 packet per slot. When the receiver has also the multi-packet reception of multi-user (MUD) detection property, by applying successive interference cancellation, IRSA also obtains very low packet loss probabilities at low traffic loads, but is unable in general to achieve a normalized throughput close to the 1. In this paper, we reconsider the case of IRSA with k -MUD receivers and derive the general density evolution equations for the non-asymptotic analysis of the packet loss rate, for arbitrary frame lengths and two variants of the first slot used for transmission. Next, using the potential function, we give new capacity bounds on the capacity of the system, showing the threshold arrival rate for zero decoding error probability. Our numerical results illustrate performance in terms of throughput and average delay for k -MUD IRSA with finite memory at the receiver, and also with bounded maximum delay.

Index Terms

Coded slotted Aloha, Density evolution, multiuser detection

I. INTRODUCTION

Simple and scalable protocols for massive random access are essential for supporting large deployments of the Internet of Things (IoT) and for large-scale machine-type communications (mMTC), as in Industry 4.0 and other specialised 5G/6G verticals [1], [2], which are starting to show an explosive commercial growth. In this context, in order to satisfy the stringent key performance targets of this type of systems in which an unknown fraction of devices out of a large collection are actively transmitting packets, the design of multiple access techniques for the next generation wireless networks has become a key enabler technology [3]. Uncoordinated transmissions on a multiple access channel (MAC) with random access and retransmissions, like in classical ALOHA [4] and variants, have very poor performance in throughput, spectral (SE) and energy efficiency (EE) when they are used in massive access conditions, since collisions waste a substantial amount of physical resources (resource blocks and energy) and may introduce large delays. This has motivated the investigation of *efficient* variants of ALOHA which keep its simplicity of operations yet can sustain high throughput and EE for IoT and mMTC applications, i.e., for low-power, low-complexity devices. Some of these grant-free novel MAC protocols have become part of standards such as NB-IoT or ETSI DVB-RCS2, and are receiving much attention as solution for next-generation MAC techniques in 5G and 6G networks [3].

A modern approach toward an efficient use of channel resources in massive MAC is to use non-orthogonal encoded transmission of packets combined with some form of successive interference cancellation (SIC) at the receiver [5], [6], [7]. In irregular repetition slotted Aloha (IRSA), the user devices transmit several replicas of each packet (an elementary form of coding by replication) in randomly selected slots. The receiver then separates the simultaneous transmissions in a given slot applying SIC: starting with some slot in which a single transmission has occurred, the receiver iteratively looks back in the past slots and attempts to cancel out the interference in those slots with collisions where a replica of the decoded packet was also transmitted. SIC removes the last decoded packet from the superposition of signals received at another slot, and this eventually enables the effective decoding of any of the replicas of other packets. The procedure can continue in the same way until no further opportunity for discovery and SIC-based decoding is detected or until all packets have been decoded. IRSA can drastically improve performance of classical ALOHA [8], [9], achieving throughput close to 1 and high EE for up to hundreds of active devices (see [10] for a modern information-theoretic formulation of massive random access). The time diversity of the packet replicas, and the system performance, is increased if each device follows a variable number of repetitions for its packets drawn from a probability distribution, which can be optimized.

Coded slotted ALOHA has been extensively studied in the literature in the asymptotic regime [7], [9] (where the packet replicas are spread over a large interval) and in the finite-length regime [11], [12], [13]. Extensions of coded ALOHA, and in particular of irregular repetition coding, to asynchronous, non-slotted RA have also been proposed and analyzed [14], [15]. Further improvement is obtained by exploiting the capture effect in wireless channels, which can be achieved by introducing transmit power diversity [16] or exploiting the natural fading, as in [17], [18], [19], or exploiting power-domain non-orthogonal signaling techniques [20]. Another form increasing the system capacity and EE of coded ALOHA is to improve the capability of the SIC-based decoder. Instead of decoding a single packet per slot, SIC can be used to attempt the recovery of up to k packets simultaneously on the same slot, by using techniques like those in power-domain non-orthogonal multiple access [3], or a pure

signal-based processing like in [21] that avoids decoding the packet symbols before the cancellation of interference. Another possibility is to equip the receiver with an user-activity detection algorithm, since multiple-packet reception is conceptually very similar to grant-free access schemes [22]. This k -MUD (multiuser detection) capability can therefore increase the probability of decoding successfully the packets, reduces the delay and enlarges the capacity of the system (up to a factor k , ideally) since several packets can be decoded at each round. However, the complexity of a k -MUD receiver is higher.

Performance analysis of IRSA and other coded ALOHA RA protocols exploits the conceptual connection between the SIC process and generalized iterative decoding of graph-based codes (e.g., low density parity-check codes (LDPC)) [23], [24], [25], [26]. There, the evolution over time of the probabilities of correct decoding of a received codeword is derived. It runs out to be a particular form of a message-passing algorithm over a bipartite graph. This density evolution (DE) forms a system of discrete dynamical equations whose fixed-point solutions yield the asymptotic error probability of the decoding process. In IRSA, a completely analogous approach can be followed for its performance analysis [6], [9], using the same tools as in graph-based coding theory, and a similar pattern of performance is obtained: the packet loss ratio (decoding failures at the SIC-receiver) follows two regimes, a waterfall region of fast, exponential decay, and an error-floor region where performance improvement practically stops. The latter is due to the existence of stopping sets in the underlying graph, i.e., the receiver reaches a trapping state where SIC cannot further proceed with the cancellation of interference. Since the analysis of the DE is complex, other works focus on the asymptotic performance exclusively, for a number of scenarios [6], or have explored alternative tools for the derivation of the asymptotic performance. A more general approach for analyzing coded RA in the asymptotic regime is the Poisson receivers framework [27], [28], which is able to capture spatial and temporal coupling among a set of receivers, including coding. However, the modeling and analysis of the DE is still of interest for deriving good approximations to finite-length systems and for gaining better insight into the design of coded ALOHA protocols, especially when the receiver uses more sophisticated strategies for SIC.

In this paper, we introduce a DE analysis of k -MUD IRSA that allows a full characterization of performance of these coded MA systems. Our approach contributes to the state-of-the-art as follows:

- We apply known tools for the derivation of the DE for k -MUD IRSA, both for the case of uniform choice of the slots for transmission of the replicas, and for the case in which the devices transmit the first replica immediately after the packet generation.
- Our results extend and improve the results in [29], [30], [31], and also provide a rigorous support to some of the examples discussed under the Poisson receivers model in [27]. These works deal mainly with the asymptotic regime and consider its stability [27] and the optimization of the degree distributions [30]. The approach in [6] relies on the classical Poisson approximation, i.e., a binomial distribution can be approximated by a properly parameterized Poisson distribution. [31] derives the density evolution only for the 2-MUD case. This work makes an exact derivation of the DE for any k .
- Unlike previous works in the literature, where the analysis focused on an asymptotically large number of slots (e.g., [32], [30], [33]), our results hold for any finite frame length n . This entails that the asymptotic behavior of the previously mentioned variants (immediate transmission in the first slot and randomized selection of the first slot) have the same performance, as expected.
- We provide new bounds to the system capacity of k -MUD IRSA. While it is known [30] that $G/k < 1$, where G is the offered traffic, we improve the known bounds.
- We show via numerical experiments that k -MUD can attain significantly better packet loss ratio and lower delay than IRSA for low values of k , without having to optimize with complex design or search the degree distributions.

The rest of the paper is organized as follows. The system model is introduced in Section II. In Section III, we present the results on the density evolution of IRSA with MUD capability. Section IV discusses the bounds on the system capacity based on our DE analysis, and Section V provides numerical performance results. The conclusions are summarized in Section VI.

II. SYSTEM MODEL

A. Irregular repetition slotted Aloha

We consider an irregular repetition Slotted Aloha (IRSA) system with a variable number of users transmitting to a common receiver, the access point (AP). In IRSA, a degree- r_u user intending to transmit a new packet selects a repetition factor r_u probabilistically, according to a predefined distribution represented by the polynomial moment generating function

$$\Lambda(x) = \sum_{i=1}^d \Lambda_i x^i, \quad (1)$$

where Λ_i is the probability of transmitting i replicas, and d is the maximum number of copies for a packet, with $\sum_{i=1}^d \Lambda_i = 1$. The average number of copies per packet is therefore $\mathbb{E}[D] = \Lambda'(1) = \sum_{i=1}^d i \Lambda_i$, where $\Lambda'(\cdot)$ is the derivative of $\Lambda(x)$. We assume that the new packets have a transmission time equal to one slot and are generated according to a Poisson process of intensity λ_a packets per slot. Thus, the number N of new packets per unit time follows a probability mass function

$$\mathbb{P}(N = j) = e^{-\lambda_a} \frac{\lambda_a^j}{j!}, \quad j = 0, 1, \dots \quad (2)$$

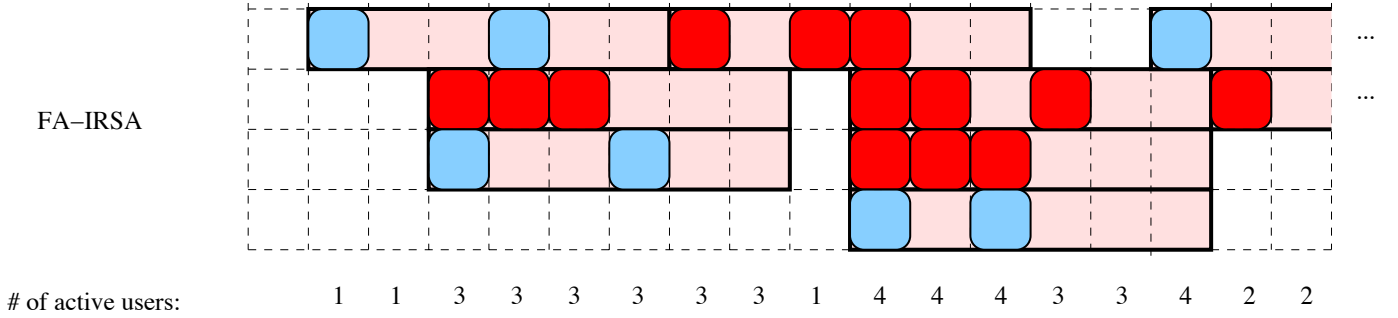


Fig. 1: An example of frame asynchronous IRSA for $n = 6$. The asynchronous system fixes the first packet copy at the first slot.

We analyze in this paper two variants of the frame asynchronous (or frameless) [14] IRSA. In both cases, all users' transmissions are arranged into frames consisting of n slots each. A degree- r_u user who joins the system at time t places its transmissions within the subsequent n slots after the packet arrival, but an active user either transmits the first replica of its new packet in the next slot, and distributes the remaining $r_u - 1$ copies randomly across the $n - 1$ subsequent slots or, alternatively, distributed its r_u replicas uniformly over the user's virtual frame $[t + 1, t + n]$, without enforcing a transmission immediately in the first slot. In all the cases, the duration n of the frames is a system-wide parameter common to all users and known to the receiver. Fig. 1 shows an example of activity in this asynchronous operation mode.

B. SIC-based Decoding

We assume the receiver has multi-user detection (MUD) capability of degree k and moreover that it adopts a successive interference cancellation (SIC) strategy for decoding. More specifically, it is assumed that, when a slot contains k or less user packets all of these can be recovered by the AP perfectly, but that decoding will fail whenever the slot has more than k active users. Note that the classical destructive collision channel model is the case $k = 1$, whereas a k -MUD receiver tolerates a certain level of interference from other users. The assumption that k is fixed also reflects well the case where all users transmit with fixed power, or when there is some form of power control enforced by the AP so that the received signals from different users have approximately equal power. The throughput and stability properties of slotted Aloha with MUD have been studied in many preceding works, e.g. [34], and an efficient form of using SIC for collision resolution in the delay domain, a natural choice for SA, is developed in [21].

If the receiver decodes successfully the packets in a slot, then it iteratively selects any other degree- k or less slot in its memory, and decodes the packets in that slot by cancelling the interference of the previously decoded packets. This process continues until no new degree- k or lower slots are found or until a maximum number of iterations is reached (to limit the memory and delay). The only difference between the synchronous and the asynchronous modes of operation is that, in the latter, the AP needs to track all the slots in the entire history of the system. So, in order to limit memory and decoding delay, a finite sliding-window of W slots is usually employed in the decoder.

The SIC-based decoding process in IRSA is entirely analogous to a message passing algorithm in a factor graph [35]. Hence, it may be modeled by a bipartite graph $\mathcal{G} = \{\mathcal{V} \cup \mathcal{C}, \mathcal{E}\}$ analogous to iterative decoding for graph-based codes [24], [13] (e.g., LDPC codes), where \mathcal{V} is the set of variable nodes in the factor graph, \mathcal{C} is the set of check or constraint nodes and \mathcal{E} are the edges connecting the variable and check nodes. For IRSA decoding, edge $(i, j) \in \mathcal{E}$ represents user i transmitting one of its replica packets in slot j . Fig. 2 depicts the graph model corresponding to the example in Fig. 1. In the graph, the colors just differentiate between users with replica factors $r_u = 2$ or $r_u = 3$. An example in which SIC-based decoding succeeds in recovering all the packets if $k \geq 2$ is shown in Fig. 3.

For the analysis of the density evolution on the underlying system graph, it is customary to introduce the enumerator polynomials

$$\Lambda(x) \triangleq \sum_{i=1}^d \Lambda_i x^i, \quad \Gamma(x) \triangleq \sum_{j=0}^{N_a} \Gamma_j x^j$$

$$\lambda(x) \triangleq \sum_{i=1}^d \lambda_i x^{i-1}, \quad \gamma(x) \triangleq \sum_{j=0}^{N_a} \gamma_j x^{j-1}$$

where Γ_j is the probability that a decoding node has degree $j = 0, \dots, N_a$; and $\lambda(x), \gamma(x)$ are the weight enumerators of the degree distributions of user and decoding nodes, respectively, from an edge perspective. Namely, λ_i denotes the probability that

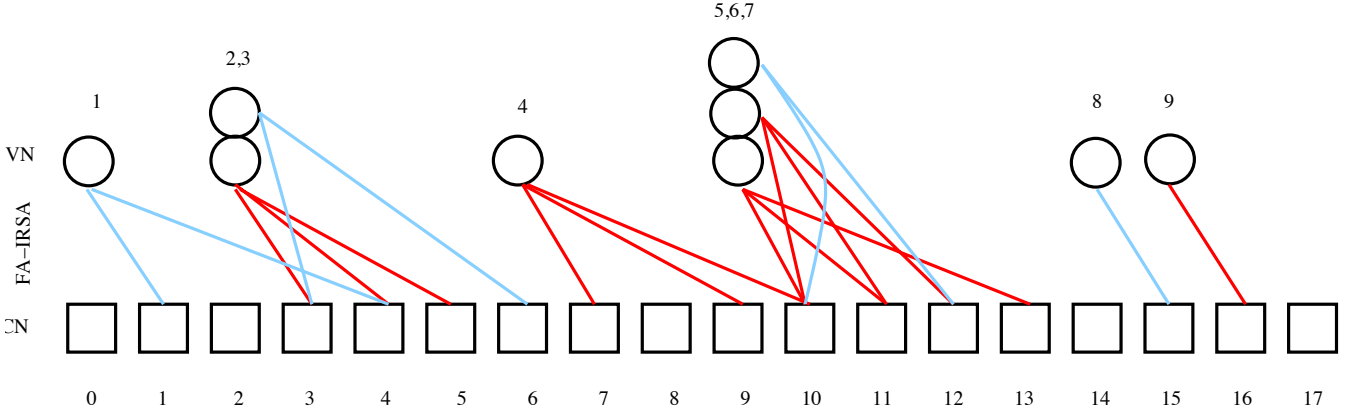


Fig. 2: Equivalent graph representation of the system depicted in Figure 3.

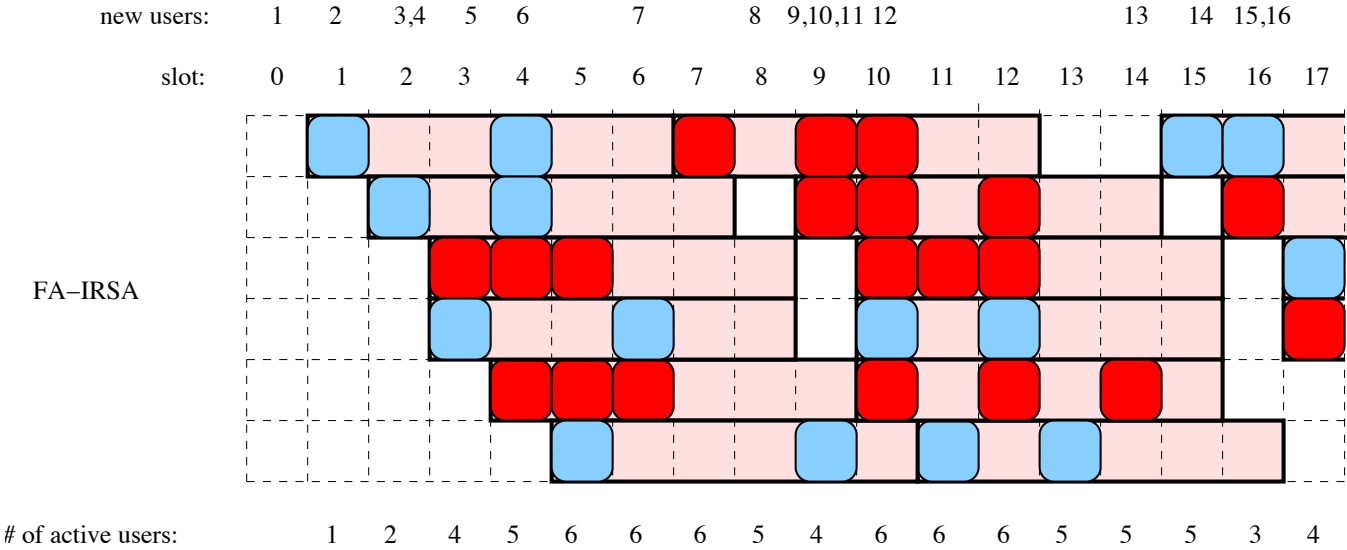


Fig. 3: An example of asynchronous IRSA with $k = 2$.

a random edge is connected to a degree- i variable node, and similarly γ_j is the probability that the random edge is connected to a degree- j check node. These probabilities are given by

$$\lambda_i = \frac{i\Lambda_i}{\sum_m m\Lambda_m}, \quad \gamma_j = \frac{j\Gamma_j}{\sum_m m\Gamma_m}. \quad (3)$$

Hence, $\lambda(x) = \Lambda'(x)/\Lambda'(1)$ and $\gamma(x) = \Gamma'(x)/\Gamma'(1)$.

The fundamental performance measures for this system are the following:

- The packet loss ratio PLR is the probability that the packet of an arbitrary users is never recovered by the SIC-based decoder.
- The delay T of a resolved packet is the number of slots between the user's arrival and the slot where the packet is resolved and correctly decoded.

III. ANALYSIS OF THE DENSITY EVOLUTION

A. Density evolution

In IRSA, packet losses arise from activity patterns that the SIC-based decoder is unable to resolve. As explained above, with slotted ALOHA these patterns are equivalent to stopping sets of LDPC codes [24], [25], so they can be analyzed with tools borrowed from the theory of codes on graphs, in particular with the density evolution (DE) technique. The DE is basically a set of fixed-point equations that describe the change over time of the probabilities $p_{(i,j)}$ ($q_{i,j}$) of the messages exchanged from a variable node (check node) to a check node (variable node) over the edge (i,j) in the factor graph. While the exact evaluation of the DE is not strictly necessary for computing the PLR in more general settings than MUD [27] (including correlated receivers or transmitters), a closed formula of the DE for a k -MUD receiver can be obtained and gives further

insights on the system performance in the asymptotic regime $n \rightarrow \infty$. Moreover, accurate approximations to the PLR can be derived from the asymptotic results once the DE is known [9], [11].

We start recalling from [9] the degree distribution of a check node at epoch $i \in \mathbb{Z}^+$, i.e., the probability distribution of the number of received packets seen by the AP in slot i .

Theorem 1 ([9], Propositions 1 and 2). *The degree distribution for a decoding node at slot $i = 1, 2, \dots$ is given by:*

(i) *For frame asynchronous IRSA with transmission of the first replica at the initial slot*

$$\Gamma^{(i)}(x) = \gamma^{(i)}(x) = \exp(-\lambda_a(1-x)), \quad i = kn \quad (4)$$

$$\Gamma^{(j)}(x) = \rho^{(j)}(x) = \exp\left(-\frac{\delta_j(\Lambda'(1)-1)}{n-1}(1-x)\right), \quad j \neq kn \quad (5)$$

where

$$\delta_j = \begin{cases} \lambda_a \min\{j-1, n-1\}, & \text{with start-up phase} \\ \lambda_a(n-1), & \text{without start-up phase,} \end{cases} \quad (6)$$

where (4) corresponds to the first slot in a frame, and (5) is for the subsequent slots in the frame.

(ii) *For frame asynchronous IRSA with uniformly distributed replicas*

$$\Gamma^{(i)}(x) = \rho^{(i)}(x) = \exp\left(-\frac{\mu_i}{n}\Gamma'(1)(1-x)\right) \quad (7)$$

where

$$\mu_i = \begin{cases} i\lambda_a, & \text{for } 1 \leq i < n \\ n\lambda_a, & \text{for } i \geq n \end{cases} \quad (8)$$

with start-up phase, and $\mu_i = n\lambda_a$ without start-up phase.

The term start-up phase refers to a system that starts totally empty, i.e., without active users and with no packets waiting to be decoded. Conversely, a system without start-up phase is supposed to be already in steady state, and analyzed thereafter. Observe from Theorem 1 that the effect of the start-up phase vanishes after n slots (one frame), so it does not have an impact on the PLR. Also, (5) differs from (4) in that the factor $\Lambda'(1) - 1 = \mathbb{E}[D] - 1$ is absent for the start-phase.

Our main result is the derivation of the density evolution of the irregular repetition slotted ALOHA with multipacket reception.

Theorem 2. *For any $i, j \geq 1$, denote by $p_{(i,i)}$, $p_{(i,j)}$, the probabilities of decoding failure of a packet replica along edges (i, i) , (i, j) at a user node. And let $q_{(i,i)}$ and $q_{(i,j)}$ be the decoding failure probabilities on edges (i, i) , (i, j) at receiver node i . The density evolution equations for the k -MUD IRSA with transmission in the first slot are given by:*

$$q_{(i,i)} = q_{(i,j)} = 1 - \sum_{m=0}^{k-1} \exp(-\nu_i) \frac{\nu_i^m}{m!} \quad (9)$$

$$p_{(i,i)} = \Gamma^{(i)}(\bar{q}_{(i,i)}) \quad (10)$$

$$p_{(i,j)} = q_{(i,i)} \gamma^{(i)}(\bar{q}_{(i,i)}) \quad (11)$$

$$\bar{q}_{(i,i)} = \frac{1}{n-1} \sum_{j=i+1}^{i+n-1} q_{(j,i)} \quad (12)$$

where $\nu_i = \lambda_a p_{(i,i)} + \frac{\Lambda'(1)}{n-1} \bar{p}_i \delta_i$ and \bar{p}_i is

$$\begin{cases} \sum_{j=1}^i \frac{p_j}{i}, & 1 \leq i < n \\ \sum_{j=i-n+1}^i \frac{p_j}{n}, & i \geq n. \end{cases} \quad (13)$$

The density evolution equations for the k -MUD IRSA with uniformly distributed replicas is given by

$$q_i = 1 - \sum_{m=0}^{k-1} \exp(-\eta_i) \frac{\eta_i^m}{m!} \quad (14)$$

$$p_i = \lambda(\bar{q}_i) \quad (15)$$

$$\bar{q}_i = \frac{1}{n} \sum_{j=i}^{i+n-1} q_j \quad (16)$$

where $\eta_i = \mu_i \bar{p}_i \Lambda'(1)/n$ and $\bar{p}_i = (\sum_{j=i-n+1}^i p_j)/n$ for $i \geq n$ or $\bar{p}_i = (\sum_{j=1}^i p_j)/i$ if $1 \leq i < n$.

Proof. See A. □

The special case $k = 1$ gives the results of pure IRSA (packet-by-packet SIC decoding) obtained previously in [9]. Note that the simultaneous decoding of k packets changes only the probability of decoding failure at the receiver nodes through (9) and (14).

REMARK The density evolution only displays minor differences between the uniformly temporally spread replicas and the use of the first slot. In functional form, (9) and (14) are equal, except for the respective arrival rates. Equations (12) and (16) are obviously identical, and the only changes between (15)-(16) and (15) arise from the deterministic use of the first slot (cf. (10)) and also from the fact that the degree distribution as seen from the user node has to be modified to account for this first transmission ($\Lambda^{(i)}$ and $\lambda^{(i)}$, respectively). Note also that the averaging of probabilities in (12) and (16) spans a window of n previous slots, where n is the frame length.

REMARK Theorem 2 gives the probabilities p_i, q_i from the node and slot perspectives *for any value of i* , not only when $i \rightarrow \infty$. The explicit dependence on the probabilities of the n previous nodes or slots is captured via the definition of the averages \bar{p}_i and \bar{q}_i . These averages obviously involve the same number of terms after the first frame, i.e., for $i > n$.

Observe that the numerical calculation for the DE in Theorem 2 involves only polynomial evaluations at each time. In the asymptotic regime $i \rightarrow \infty$, we obtain the PLR of k -MUD IRSA as an immediate consequence of the latter Theorem.

Corollary 1. *The packet loss ratio of k -MUD IRSA at receiver node i is*

(i) *With first slot fixed*

$$\bar{p}_i = \Lambda(\bar{q}_i)q_{(i,i)}/\bar{q}_i; \quad (17)$$

(ii) *and with uniformly distributed replicas*

$$\bar{p}_i = \Lambda(\bar{q}_i). \quad (18)$$

The asymptotic PLR is $\text{PLR} = \lim_{i \rightarrow \infty} \bar{p}_i$.

In practice, the PLR can be computed as the fixed-point solution of (9)-(12) or (14)-(16), respectively, setting initially all the edge probabilities to 1.

B. Potential function and stability

For $i \gg n$, the density evolution for asynchronous IRSA converges to unique values p, q , independent of the slot position i , which are the solution to the fixed point equation

$$x = \Lambda(g_k(x)) \quad (19)$$

where

$$g_k(x) = 1 - \exp(-\zeta x) \sum_{j=0}^{k-1} \frac{(\zeta x)^j}{j!}, \quad (20)$$

$\zeta \triangleq \lambda_a \Lambda'(1)$, and λ_a is the arrival rate of transmitters per slot. Recall from Theorem 2 that

$$p_i = \Lambda\left(1 - \exp(-\eta_i) \sum_{m=0}^{k-1} \frac{\eta_i^m}{m!}\right) \quad (21)$$

and $\eta_i = \lambda_a \bar{p}_i (\Lambda'(1) - 1)$, where \bar{p}_i is the average of $\{p_i\}$ over the last n slots. The mapping $\eta_i \rightarrow T(\eta_i) := \exp(-\eta_i) \sum_{m=0}^{k-1} \eta_i^m / m!$ is continuous and increasing, and has $T(0) = 1$. Assume now that $p_{i+1} \leq p_i$ for all $i < s$. Then $\eta_{s+1} \leq \eta_s$ since the average \bar{p}_i is non-increasing, and

$$p_{s+1} = \lambda(1 - T(\eta_s)) \leq \lambda(1 - T(\eta_{s-1})) = p_s \quad (22)$$

where the inequality follows since $\lambda(x)$ is increasing in $x \in [0, 1]$, $\eta_s \leq \eta_{s+1}$ and the assumption that $T(\cdot)$ is continuous and increasing. Therefore, the sequence $\{p_s\}$ and its average \bar{p}_s converge to a limit $p^* \geq 0$ which is necessarily a fixed point of the DE.

In the context of graph-based codes analyzed through the DE technique, the potential function is defined as [24]

$$U(x) := xg(x) - G(x) - F(g(x)) \quad (23)$$

where $G(x) := \int_0^x g(z)dz$ and $F(x) = \int_0^x \lambda(z)dz$. Recalling that $\lambda(x) = \Lambda'(x)/\Lambda'(1)$, we have $F(x) = (\Lambda(x) - \Lambda(0))/\Lambda'(1) = \Lambda(x)/\Lambda'(1)$. The usefulness of this function for the stability of the system comes from the fact that

$$\lambda_a^* = \sup(\lambda_a : U'(x) > 0 \forall x \in [0, 1]) \quad (24)$$

is the threshold for the feasible arrival rates, i.e, the supremum of the arrival rates such that $\text{PLR} = \lim_{i \rightarrow \infty} p_i = 0$.¹ Note that for computing λ_a^* we can use $\tilde{F}(x) = \Lambda(x)/\Lambda'(1)$ in the definition of the potential function. The closed-form expression for the potential function in k -MUD IRSA is given in the following theorem.

Theorem 3. *The potential function for k -MUD frame asynchronous IRSA with is given by*

$$U_k(x) = k - \frac{1}{\zeta} \exp(-\zeta x) \sum_{j=0}^{k-1} \frac{(\zeta x)^j}{j!} (\zeta x + k - j) - \frac{\Lambda(g_k(x))}{\Lambda'(1)} \quad (25)$$

where $\zeta \triangleq \lambda_a \Lambda'(1)$ and $g_k(x)$ is given in (20).

Proof. First, consider the function $g_k(x)$ in (20). Integrating by parts each of the terms in the sum we get

$$I_j(x) \triangleq \int_0^x \exp(-\zeta t) \frac{(\zeta t)^j}{j!} dt = I_{j-1}(x) - \frac{1}{\zeta} \exp(-\zeta x) \frac{(\zeta x)^j}{j!} = \dots = I_0(x) - \frac{1}{\zeta} \exp(-\zeta x) \sum_{m=1}^j \frac{(\zeta x)^m}{m!}$$

Using that $I_0(x) = 1 - 1/\zeta \exp(-\zeta x)$ we obtain

$$I_j(x) = 1 - \frac{1}{\zeta} \exp(-\zeta x) \sum_{m=0}^j \frac{(\zeta x)^m}{m!}$$

and thus

$$G(x) = x - \sum_{j=0}^{k-1} I_j(x) = x - k + \frac{1}{\zeta} \exp(-\zeta x) \sum_{j=0}^{k-1} \sum_{m=0}^j \frac{(\zeta x)^m}{m!} = x - k + \frac{1}{\zeta} \exp(-\zeta x) \sum_{j=0}^{k-1} (k - j) \frac{(\zeta x)^j}{j!},$$

where the last equality follows after exchanging the order of the summations. Now, since

$$xg_k(x) = x - \frac{1}{\zeta} \exp(-\zeta x) \sum_{j=0}^{k-1} \frac{(\zeta x)^{j+1}}{j!}$$

we have

$$U_k(x) = xg_k(x) - G(x) - F(g_k(x)) = k - \frac{1}{\zeta} \exp(-\zeta x) \sum_{j=0}^{k-1} \frac{(\zeta x)^j}{j!} (\zeta x + k - j) - \frac{\Lambda(g_k(x))}{\Lambda'(1)}.$$

This finishes the proof. \square

The special case $k = 1$ yields the formula

$$U_1(x) = 1 - \frac{\zeta x + 1}{\zeta} \exp(-\zeta x) - \frac{\Lambda(g_1(x))}{\Lambda'(1)}. \quad (26)$$

In Figure 4 we show an example of the potential function for the k -MUD IRSA with uniform slot selection, for two degree distributions $\Lambda(x) = 0.86x^3 + 0.14x^8$ and $\Lambda(x) = x^5$, and $k = 3$, as a function of the arrival rate λ_a . Visually, the threshold $\lambda^* \approx 2$ for the first case, and is approximately 1.65 for the latter case.

IV. CAPACITY BOUNDS

Theorem 3 provides a closed-form expression for the potential function. In principle, one could use it for determining analytically the maximum arrival rate λ_a^* to the system, simply by finding whether the maximum of $U_k(x)$ is attained in $(0, 1)$ or not. Using (24), one can conclude that the arrival rate λ_a is feasible for decoding without error if $\lambda(g_k(x)) < x$ for all $x \in (0, 1)$. In fact, a direct calculation from Theorem 3 arrives at the same conclusion.

Lemma 1. *The maximum of the potential function $U_k(x)$ is the solution to*

$$\lambda(g_k(x)) = x.$$

Proof. See B. \square

This simple result can be used in two ways. First, we can use the expression in the Lemma by expanding the term $\lambda(g_k(x))$ as a power series in the variable x and equate the terms in the RHS and the LHS so that the LHS is less than λ_a^{-1} for any $x \in (0, 1)$. This would imply that the potential function is increasing in the interval, hence the arrival rate λ_a is feasible for

¹Recall that the PLR accounts for the decoding errors with SIC, exclusively. We do not include in the model the possibility of transmission errors for simplicity.

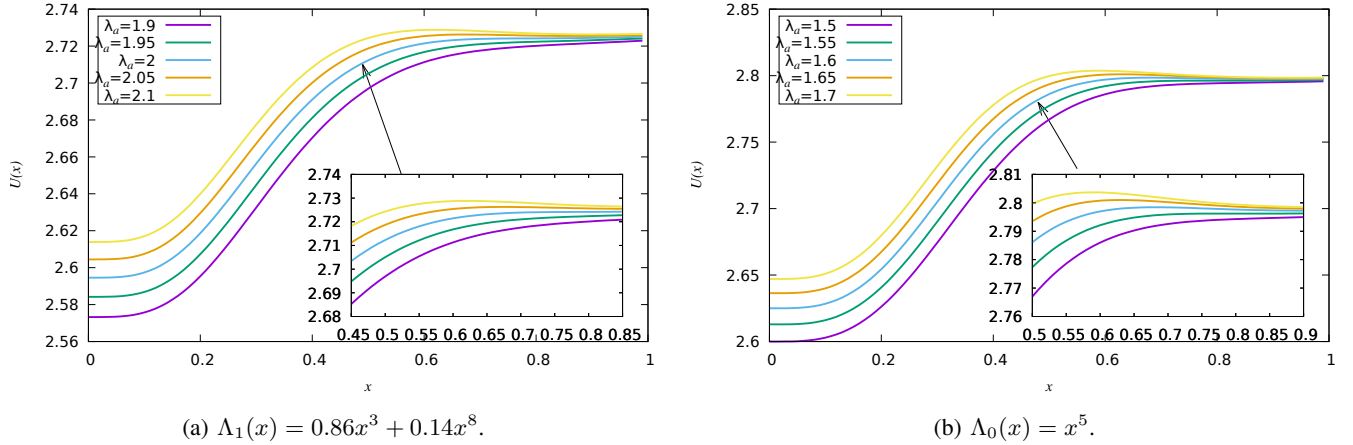


Fig. 4: Examples of the potential function for FA-IRSA with uniform slot selection vs. users arrival rate λ_a ; $k = 3$.

TABLE I: Simulation parameters used for performance analysis.

PARAMETER	VALUES
Degree distributions	$\Lambda_0(x) = x^5$ $\Lambda_1(x) = 0.86x^3 + 0.14x^8$ $\Lambda_2(x) = 0.8793x^2 + 0.003x^7 + 0.1204x^{11}$ $\Lambda_3(x) = 0.929x^2 + 0.07x^{11}$
k	{1, 2, 3}
n (slots)	{50, 100, 150, 200, 300, 400}

some degree distribution $\Lambda(x)$ which is the solution to a set of *linear* equations. In other words, it is possible to use the result of the Lemma to synthesize optimal degree distributions just by solving numerically a few linear equations under the constraints that $\sum_i \lambda_i = 1$ and $\lambda_i \geq 0$. This improves the method described in [30], where a linear program has to be solved for the same purpose. We can further note that the optimal distributions are of the form $\lambda(x) = o(x)$ (see [30], [9]). This implies that the solution to the functional equation $\lambda(g_k(x)) = x$ is bounded away from zero, since otherwise, as $g_k(x) = o(x^k)$, we would have $o(x^{k+1}) = o(1)$, which is not possible for $k \geq 1$. A similar argument shows that the root is also bounded away from 1, since $\lambda(x)$ is a convex polynomial, hence it is a superadditive function and

$$\lambda(g_k(x)) + \lambda(1 - g_k(x)) \leq \lambda(g_k(x) + 1 - g_k(x)) = \lambda(1) = 1, \quad (27)$$

hence $\lambda(1 - g_k(x)) \leq 1 - \lambda(g_k(x))$.

In [30], it is shown that a lower bound for $\lambda_a - k$ is given by

$$E = \int_0^{s_k} (F_k^{-1}(x) - \alpha_k x) dx, \quad (28)$$

where $F_k(x) = 1 - \sum_{i=0}^{k-1} x^i/i!$, and α_k is the root of $F_k^{-1}(x) - (F_k^{-1})'(x)x = 0$. A direct calculation yields

$$E = \exp(-y) \sum_{i=0}^{k-1} \frac{(k-i)y^i}{i!} + \frac{y}{2} F_k(y) \quad (29)$$

where $\alpha_k = F_k(y)$.

V. NUMERICAL RESULTS

In this Section, we investigate the performance of k -MUD IRSA through numerical experiments. Specifically, we consider the packet loss ratio and the decoding delay for several illustrative degree distributions of the replica process at the transmitters, $\Lambda_0(x) = x^5$, $\Lambda_1(x) = 0.86x^3 + 0.14x^8$ and $\Lambda_2(x) = 0.8793x^2 + 0.003x^7 + 0.1204x^{11}$, and $\Lambda_3(x) = 0.929x^2 + 0.07x^{11}$. The first is a regular repetition pattern, since it generates exactly 5 replicas per packet, and this will allow us to test the impact of sparsity on the performance metrics; the second one was used in [13]. It is not optimal, but provides a high threshold for a probability at the error floor around 10^{-5} ; $\Lambda_3(x)$ was derived in [30] numerically as the optimal distribution for $k = 2$; $\Lambda_4(x)$ was also found in [30] as the optimal distribution for $k = 3$ with degree less than or equal to 11. Table I summarizes the configuration parameters used in the tests. All our results are given as a function of the normalized system load $L = \lambda_a/k \in [0, 1]$ to make the comparison among different values of k easier.

We start our numerical experiments by computing the asymptotic iterative decoding thresholds separating the waterfall and error-floor regions. These thresholds provide a simple numerical characterization of the system stability. Figure 5 confirms the

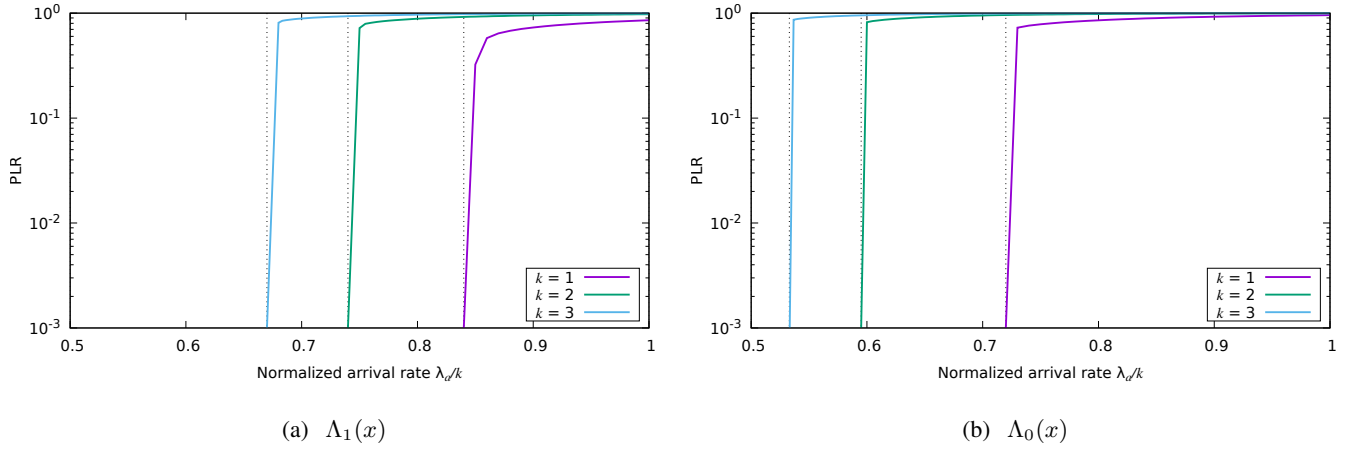


Fig. 5: Decoding thresholds for MUD IRSA, $k = 1, 2, 3$.

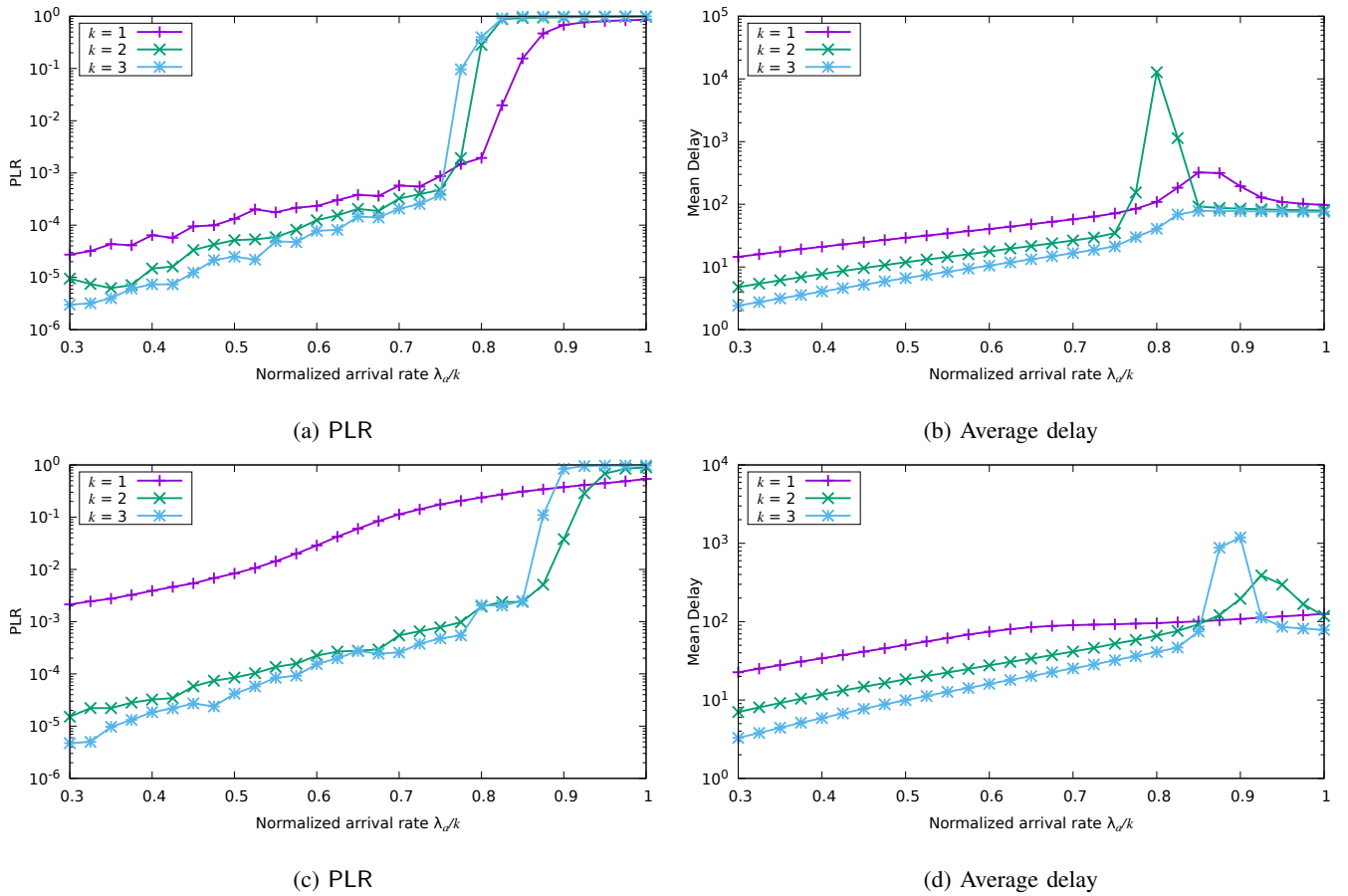


Fig. 6: Simulation. Performance for $\Lambda_1(x)$ and $\Lambda_2(x)$, frame length $n = 200$ slots.

substantial benefits or irregular repetition (case (a)) over a constant factor for the replicas (case (b)), but also show that the threshold λ_a^* is sublinear in k , suggesting that the use of higher values of k has a marginally decreasing improvement. Thus, we limit our experiments to low values of k in the remaining tests, as listed in Table I.

A. Packet Loss Rate and Average Delay: finite frame length

The PLR and the average delay are simulated and depicted in Fig. 6. As the figure shows, the PLR is decreasing in k for the same normalized load L , and the average decoding delay is consistently lower as k increases when L is below the asymptotic decoding threshold, as expected (the decoding delay is measured in number of slots). There is a phase transition clearly seen around that threshold, corresponding to the system entering into the waterfall regime, in which the receiver starts

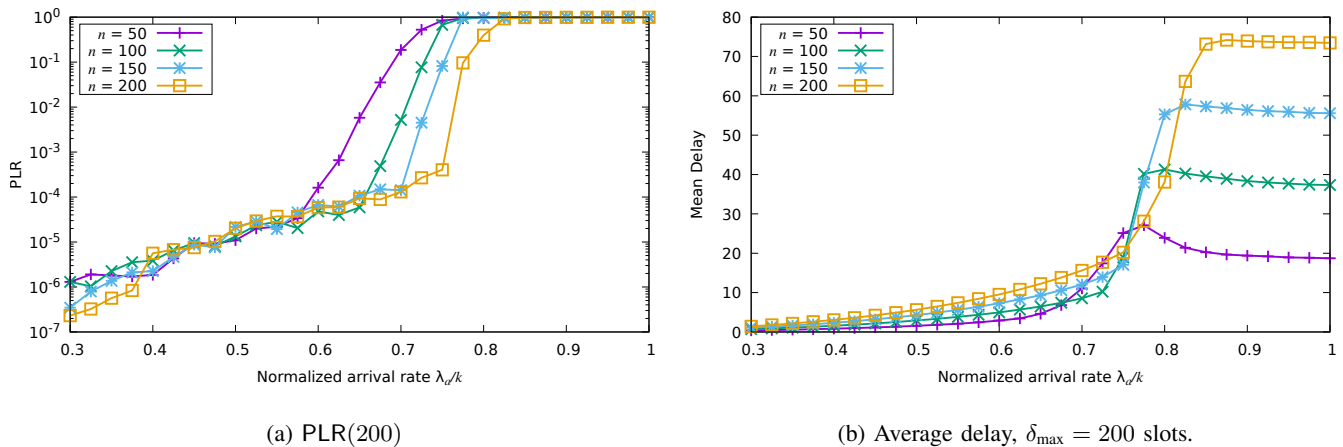


Fig. 7: Performance for 3-MUD IRSA with bounded delay, $\delta_{\max} = 200$ slots. Degree distribution $\Lambda_1(x)$.

to be unable to decode some packets, or achieves that only after a long delay. This explains the increase in decoding delay, which is particularly sharp for $k = 2$. Once L is beyond the threshold, PLR increases quickly, so the receiver discards a fraction of the packets and those which can actually be correctly decoded have a decoding delay almost independent of L . These results are also observed for the case without irregular repetition (Fig. 6, (c)-(d)), with the difference that the end of the waterfall region occurs at $L \approx 0.9$ instead of $L \approx 0.8$ for the distribution $\Lambda_1(x)$. We also see that, below the threshold, the average decoding delay appears to be linear in L , and that the limiting average decoding delay when $L \rightarrow 1$ is virtually independent of k and approximately equal to $n/2$.

B. PLR and Average Delay with Maximum Delay Constraint

The last Section showed simulation results for a receiver with unbounded delay, i.e., all the received replicas are kept into memory awaiting for a decoding opportunity. This was done only for the purpose of obtaining the lowest possible PLR, by not missing any packet decoding event except those due to stopping sets in the underlying decoding graph. For real systems, k -MUD will be limited either by a maximum delay constraint or by the maximum amount of memory at the receiver. Thus, we present here the performance under the first assumption, a maximum delay constraint δ_{\max} . The packet loss ratio in this case $\text{PLR}(\delta_{\max})$ is defined as the probability that a packet of an arbitrary users is not successfully resolved within δ_{\max} slots after the user transmits its first replica packet. Note that the delay constraint does not imply a bound on the memory used at the receiver, especially for large loads. We will analyze the setup with finite memory in a subsequent Section.

The results are shown in Fig. 7. We clearly see that increasing the frame length under the constraint of maximum delay shifts the PLR threshold to the right, as shown in panel (a), at the cost of a greater average delay (panel (b)). Again, around the threshold point the delay increases quickly up to its saturation point, which is in all the experiments under half the frame length. One of the advantages of multipacket detection is that, for low or moderate L , the average delay and the PLR are significantly lower than in the classical collision model (Fig. 8). These observations also hold for the case of other distributions, as displayed in Fig. 8(c)-(d), and (e)-(f).

C. PLR Loss Rate and Mean Delay with Maximum Memory Constraint

Instead of enforcing a maximum delay, a more natural constraint to reduce the complexity of the receiver is to limit the amount of memory used to hold the received packets while awaiting for a decoding opportunity. A small memory size is desirable, but it might lead to miss the decoding of some packets when the traffic load is high. To explore this trade-off, we have simulated the system using a fixed amount of memory $n_{\max} = 400$ packets (we consider each replica a different packet for counting the memory use). Figure 9 collects the results for comparison of pure IRSA ($k = 1$, top), 2-MUD (middle), and 3-MUD, 2-MUD (bottom) in this respect.

VI. CONCLUSIONS

Introducing the capability of multipacket reception into uncoordinated wireless communications improves the system utilization and its energy efficiency, simultaneously, contributing to a scalable solution able to support tens to hundreds of devices, as in IoT and mMTC applications. We derived in this paper the dynamic density evolution equations for performance analysis of IRSA with k -MUD at the SIC receiver(s). Unlike previous works in the literature, where the analysis focused on an asymptotically large number of slots, our results hold for the finite length regime. The expressions are tractable due to the memoryless property of the Poisson distribution, and involve only modified terms to account for the effective decoding probability at each

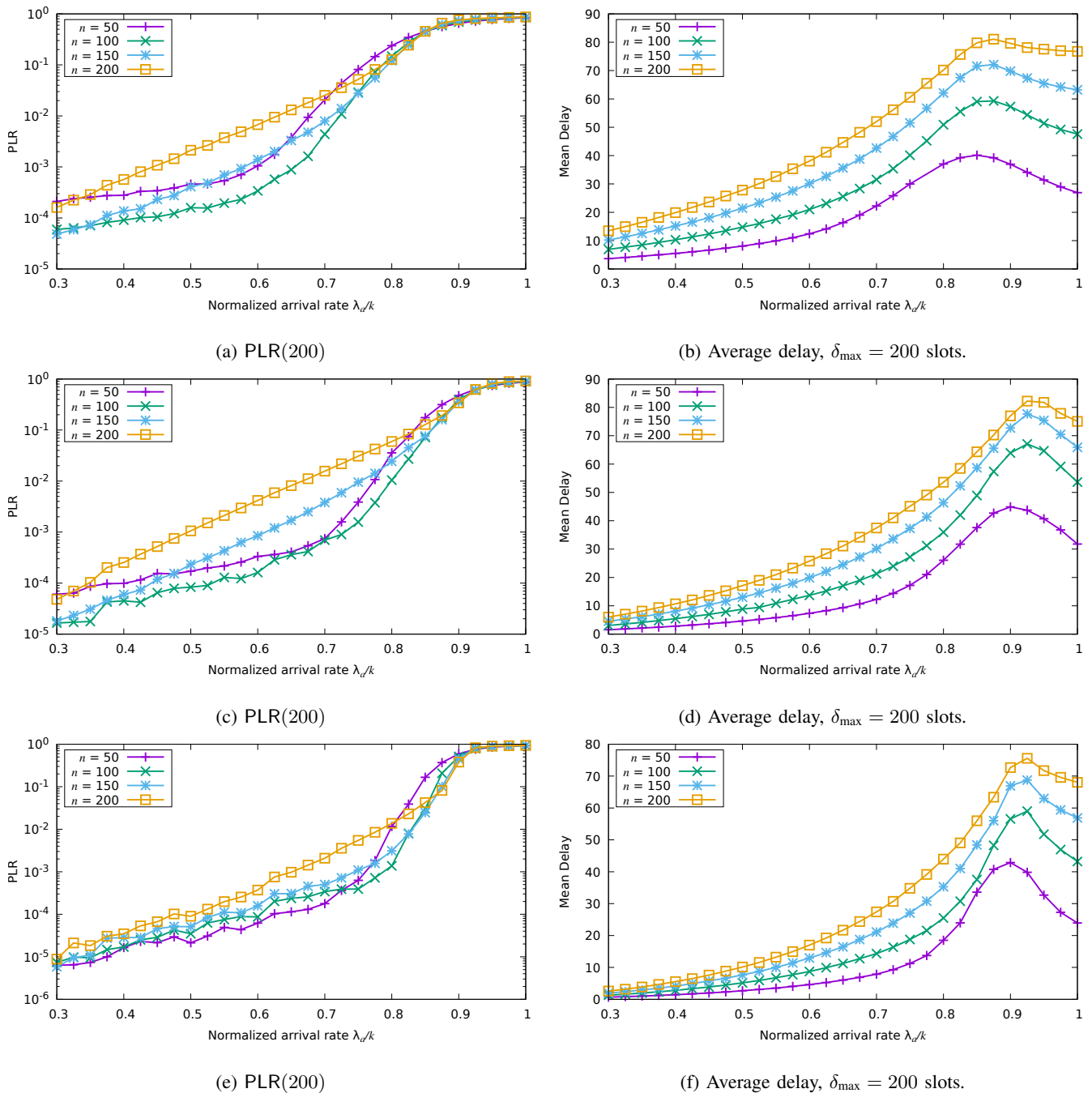
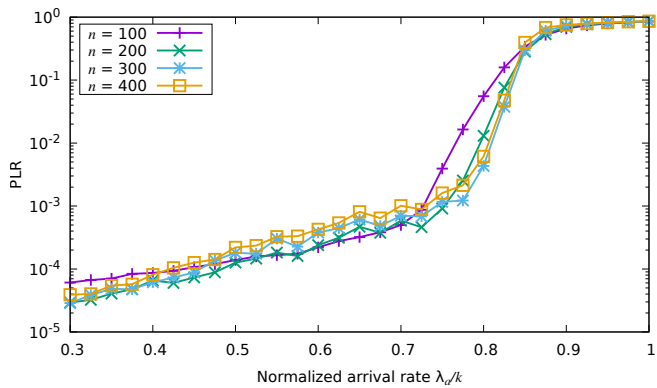
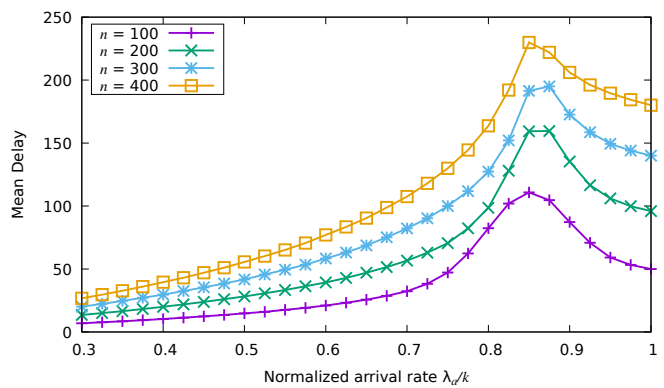
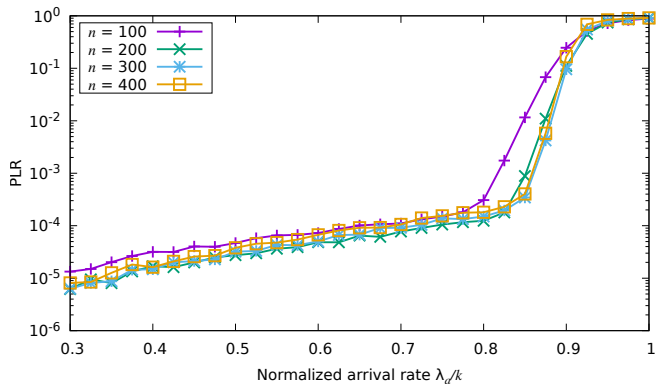


Fig. 8: Performance for IRSA with bounded delay, $\delta_{\max} = 200$ slots. Degree distributions $\Lambda_1(x)$ in (a)-(b); $\Lambda_2(x)$ in (c)-(d); $\Lambda_3(x)$ in (e)-(f).

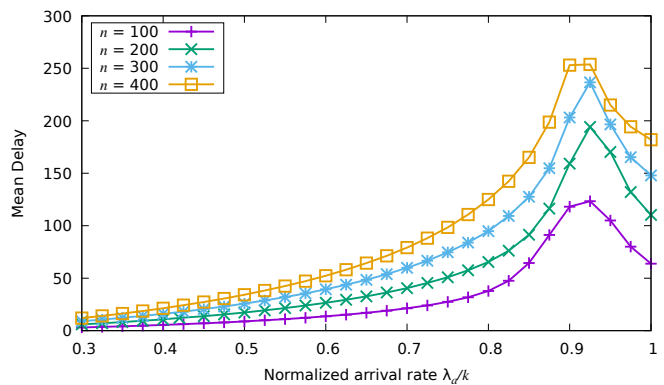
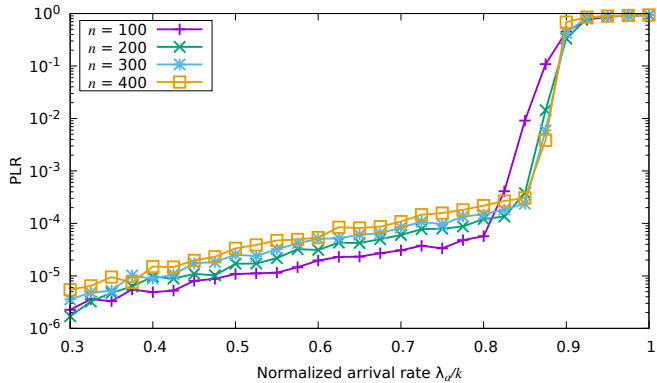
time slot at the receiver. This density evolution approach can be used to calculate the associated potential function and the decoding threshold for IRSA, and provides a benchmark for numerical approximations to the error floor probability like those developed in [6], [15]. Our simulation results quantify the effects of MUD, finite memory and/or bounded maximum delay at the decoder, and show that MUD does not require, in general, long frame lengths nor excessive memory to perform well up to high normalized traffic loads. These observations emphasize the importance of introducing SIC in IRSA receivers, even to a low degree. The present work can be extended in several directions. One obvious direction is to consider more realistic model for SIC and analyze the robustness of the schemes against channel impairments, power control, or CSIT estimation. Another possibility is to use the framework to optimize the degree distribution of IRSA in terms of signal-to-noise ratio, offered load, and rate.



(a) PLR

(b) Average delay, $n_{\max} = 400$ slots.

(c) PLR

(d) Average delay, $n_{\max} = 400$ slots.

(e) PLR

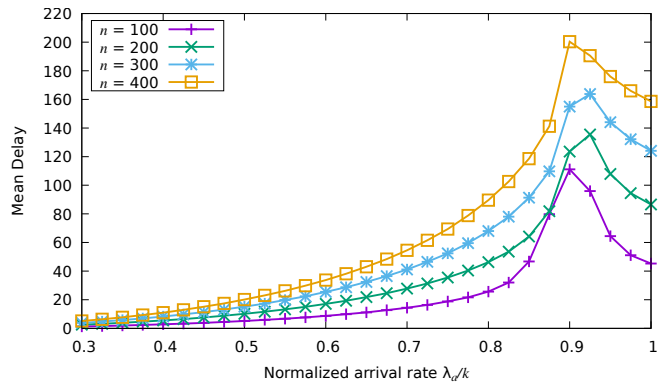
(f) Average delay, $n_{\max} = 400$ slots.

Fig. 9: Performance for IRSA with bounded memory, $n_{\max} = 400$ slots. Degree distributions $\Lambda_1(x)$ in (a)-(b); $\Lambda_2(x)$ in (c)-(d); $\Lambda_3(x)$ in (e)-(f).

VII. ACKNOWLEDGMENTS

This work was supported by the Spanish Government under grants “Enhancing Communication Protocols with Machine Learning while Protecting Sensitive Data (COMPROMISE)” PID2020-113795RB-C33, and ICARUS “Red satelital centrada en información para comunicaciones vehiculares” PID2020-113240RB-I00, funded by MCIN/AEI/10.13039/501100011033.

APPENDIX

The proof is divided in two cases. The system with fixed transmission in the first slot of the user’s virtual frame is more involved and is addressed first. The proof technique is the same for uniform distribution of the packet replicas in IRSA. The key property is that the messages that arrive at a user or receiver node are a thinned Poisson process that depends on the previous density values in a sliding window of length n and on the degree distributions.

A. Density evolution with transmission in the first slot

Suppose the first replica is sent always in the first slot after its arrival to the system. Then, a variable node at epoch i is always connected to the check node at epoch i , while the remaining edges are connected to other future positions randomly chosen. Thus, there are two different edge types and the density evolution involves the quantities $p_{(i,i)}$, $p_{(i,j)}$, $q_{(i,i)}$ and $q_{(i,j)}$ for the probabilities of the messages exchanged between user nodes and receiver nodes (see again Figure 1). The subscripts make clear the orientation and type of the edges.

Let us derive first $p_{(i,i)}$ and $p_{(i,j)}$, the probabilities of decoding failures in edges (i,i) and (i,j) , seen from a user node. An outgoing message from user node i fails if all of its incoming messages also fail, i.e., if there is no slot such that the replica can be successfully decoded. Suppose the user node has degree r and is at position i , so it has an edge to the receiver node at position i and other $r-1$ edges at positions beyond i . Since the edges that connect the user node to the receiver nodes are drawn uniformly from the interval $[i+1, i+n-1]$ the average incoming failure probability along each edge is the same, and is given by

$$\bar{q}_{(i,i)} := \frac{1}{n-1} \sum_{j=i+1}^{i+n-1} q_{(j,i)}. \quad (30)$$

Thus, the probability that the message sent along (i,i) is an erasure is $\bar{q}_{(i,i)}^{r-1}$, and averaging over the degree distribution $\Lambda^{(i)}(x)$, we get

$$p_{(i,i)} = \sum_r \Lambda_r^{(i)} \bar{q}_{(i,i)}^{r-1} := \Lambda^{(i)}(\bar{q}_{(i,i)}). \quad (31)$$

In an analogous way, $p_{(i,j)}$ can be obtained as

$$p_{(i,j)} = q_{(i,i)} \sum_r \lambda_r^{(i)} \bar{q}_{(i,i)}^{r-2} = q_{(i,i)} \lambda^{(i)}(\bar{q}_{(i,i)}) \quad (32)$$

for $j \in [i+1, i+n-1]$.

The derivation of the probabilities $q_{(i,i)}$ and $q_{(i,j)}$ can be done as follows. With k -MUD, an edge outgoing from receiver node i is a decoding failure if at least k of its incoming edges (distinct from the outgoing edges) fail. This is because the receiver can decode perfectly any slot with k or less packets, so only slots with more than k packets are unsuccessful. Conversely, a message from a receiver node is not a failure if less than k of its other $r_1 + r_2 - 1$ incoming edges are erasures. Consider a receiver node of degree r at position i , say w . Node w has r_1 edges connected to type i user nodes, and r_2 edges connected to nodes in the time window

$$\mathcal{J}_i = \begin{cases} \emptyset, & \text{for } i = 1 \\ [1, i-1], & 2 \leq i < n \\ [i-n+1, i-1], & i \geq n. \end{cases} \quad (33)$$

Then the (conditional) probability that an outgoing message along an edge e connecting w to a variable node of type i is a failure, p_e , is the probability that k_1 of the remaining $r_1 - 1$ edges connecting w to type i variable nodes, and k_2 out of the r_2 edges connecting w to some variable node in \mathcal{J}_i are all failures, for any pair (k_1, k_2) such that $k_1 + k_2 \geq k$. Hence

$$p_e = \sum_{k_1+k_2 \geq k} \binom{r_1-1}{k_1} p_{(i,i)}^{k_1} (1-p_{(i,i)})^{r_1-1-k_1} \binom{r_2}{k_2} \bar{p}_i^{k_2} (1-\bar{p}_i)^{r_2-k_2} \quad (34)$$

where it must be understood that $\binom{a}{b} = 0$ if $a < b$. The particular case $k = 1$, i.e., without MUD, gives $1 - p_e = (1 - p_{(i,i)})^{r_1-1} (1 - \bar{p}_i)^{r_2}$. In the above formulas

$$\bar{p}_i = \begin{cases} 0, & \text{for } i = 1 \\ \sum_{k \in \mathcal{J}_i} p_{(k,i)} / (i-1), & \text{for } 1 < i < n \\ \sum_{k \in \mathcal{J}_i} p_{(k,i)} / (n-1), & \text{for } i \geq n \end{cases} \quad (35)$$

is the average failure probability of incoming messages from user nodes in the time interval \mathcal{J}_i . Now, we average (34) over the edge-perspective receiver node distribution and the node-perspective receiver node distribution, jointly. We have

$$q_{(i,i)} = \mathbb{E}_{r_1 \sim \gamma^{(i)}} \mathbb{E}_{r_2 \sim \Gamma^{(i)}} \left[\sum_{k_1+k_2 \geq k} \binom{r_1-1}{k_1} p_{(i,i)}^{k_1} (1-p_{(i,i)})^{r_1-1-k_1} \binom{r_2}{k_2} \bar{p}_i^{k_2} (1-\bar{p}_i)^{r_2-k_2} \right] \quad (36)$$

$$= \sum_{r_1, r_2} \mathbb{P}(\gamma^{(i)} = r_1) \mathbb{P}(\Gamma^{(i)} = r_2).$$

$$\sum_{k_1+k_2 \geq k} \binom{r_1-1}{k_1} p_{(i,i)}^{k_1} (1-p_{(i,i)})^{r_1-1-k_1} \quad (37)$$

$$\binom{r_2}{k_2} \bar{p}_i^{k_2} (1-\bar{p}_i)^{r_2-k_2}. \quad (38)$$

Interchanging the outer and inner summations this can be rearranged as

$$q_{(i,i)} = \sum_{k_1+k_2 \geq k} \left(\sum_{r_1=1}^{\infty} \mathbb{P}(\gamma^{(i)} = r_1) \binom{r_1-1}{k_1} p_{(i,i)}^{k_1} (1-p_{(i,i)})^{r_1-1-k_1} \right) \cdot \left(\sum_{r_2=0}^{\infty} \mathbb{P}(\Gamma^{(i)} = r_2) \binom{r_2}{k_2} \bar{p}_i^{k_2} (1-\bar{p}_i)^{r_2-k_2} \right). \quad (39)$$

Now, for the first sum

$$\begin{aligned} & \sum_{r_1=1}^{\infty} \mathbb{P}(\gamma^{(i)} = r_1) \binom{r_1-1}{k_1} p_{(i,i)}^{k_1} (1-p_{(i,i)})^{r_1-1-k_1} \\ &= \sum_{r_1=0}^{\infty} \exp(-\lambda_a) \frac{\lambda_a^{r_1}}{r_1!} \binom{r_1}{k_1} p_{(i,i)}^{k_1} (1-p_{(i,i)})^{r_1-k_1} \end{aligned} \quad (40)$$

$$\begin{aligned} &= \frac{(\lambda_a p_{(i,i)})^{k_1}}{k_1!} \exp(-\lambda_a) \sum_{r_1=0}^{\infty} \frac{(\lambda_a (1-p_{(i,i)}))^{r_1}}{r_1!} \\ &= \exp(-\lambda_a p_{(i,i)}) \frac{(\lambda_a p_{(i,i)})^{k_1}}{k_1!} \end{aligned} \quad (41)$$

where equality (40) follows from the fact that $\gamma_{r_1}^{(i)} = \Gamma_{r_1-1}^{(i)}$ and the arrivals are Poissonian, and (41) follows because $\sum_{n=0}^{\infty} x^n/n! = \exp(x)$. For the second term, using Theorem 1 and the fact that $\Gamma^{(i)}$ follows a Poisson distribution

$$\begin{aligned} & \sum_{r_2=0}^{\infty} \mathbb{P}(\Gamma^{(i)} = r_2) \binom{r_2}{k_2} \bar{p}_i^{k_2} (1-\bar{p}_i)^{r_2-k_2} \\ &= \sum_{r_2=0}^{\infty} \binom{r_2}{k_2} \bar{p}_i^{k_2} (1-\bar{p}_i)^{r_2-k_2} \exp(-z\delta_i) \frac{(z\delta_i)^{r_2}}{r_2!} \\ &= \frac{(z\bar{p}_i\delta_i)^{k_2}}{k_2!} \exp(-z\bar{p}_i\delta_i) \end{aligned} \quad (42)$$

where $z = (\Lambda'(1) - 1)/(n - 1)$. Using (41) and (42) in (39) we have

$$q_{(i,i)} = \sum_{k_1+k_2 \geq k} \exp(-\lambda_a p_{(i,i)} - z\bar{p}_i\delta_i) \frac{(\lambda_a p_{(i,i)})^{k_1}}{k_1!} \frac{(z\bar{p}_i\delta_i)^{k_2}}{k_2!} = \mathbb{P}(V_1 + V_2 \geq k) \quad (43)$$

where $V_1 \sim \text{Poisson}(\lambda_a p_{(i,i)})$, $V_2 \sim \text{Poisson}(z\bar{p}_i\delta_i)$ and V_1, V_2 are independent random variables. Since the sum of independent Poisson variables is Poisson, we finally conclude

$$q_{(i,i)} = 1 - \sum_{m=0}^{k-1} \exp(-\nu_i) \frac{\nu_i^m}{m!} \quad (44)$$

with $\nu_i \triangleq \lambda_a p_{(i,i)} + z\bar{p}_i\delta_i = \lambda_a p_{(i,i)} + (\Lambda'(1) - 1)/(n - 1)\bar{p}_i\delta_i$.

In a similar way, the probability $q_{(i,j)}$ can be derived after averaging

$$\sum_{k_1+k_2 \geq k} \binom{r_1}{k_1} p_{(i,i)}^{k_1} (1-p_{(i,i)})^{r_1-k_1} \binom{r_2-1}{k_2} \bar{p}_i^{k_2} (1-\bar{p}_i)^{r_2-1-k_2} \quad (45)$$

over the node-perspective and the edge-perspective receiver node degree distributions, i.e.

$$q_{(i,j)} = \mathbb{E}_{r_2 \sim \gamma^{(i)}} \mathbb{E}_{r_1 \sim \Gamma^{(i)}} \left[\sum_{k_1+k_2 \geq k} \binom{r_1}{k_1} p_{(i,i)}^{k_1} (1-p_{(i,i)})^{r_1-k_1} \binom{r_2-1}{k_2} \bar{p}_i^{k_2} (1-\bar{p}_i)^{r_2-1-k_2} \right] \quad (46)$$

$$\begin{aligned} &= \sum_{r_1=0}^{\infty} \sum_{r_2=1}^{\infty} \mathbb{P}(\gamma^{(i)} = r_2) \mathbb{P}(\Gamma^{(i)} = r_1) \cdot \\ &\quad \left(\sum_{k_1+k_2 \geq k} \binom{r_1}{k_1} p_{(i,i)}^{k_1} (1-p_{(i,i)})^{r_1-k_1} \binom{r_2-1}{k_2} \bar{p}_i^{k_2} (1-\bar{p}_i)^{r_2-1-k_2} \right). \end{aligned} \quad (47)$$

Noting that (34) and (45), and also (36) and (46) are the same if we swap indices 1 and 2, we obtain

$$q_{(i,j)} = q_{(i,i)} = 1 - \sum_{m=0}^{k-1} \exp(-\nu_i) \frac{\nu_i^m}{m!}. \quad (48)$$

Equality follows from the fact that $\Gamma^{(i)}(x) = \gamma^{(i)}(x)$ which is in turn a consequence of the underlying Poisson distributions. This proves part (i) in Theorem 2. Notice that (48) is independent of j .

B. Density evolution with uniformly distributed replicas

When the slots for transmitting the replicas are chosen uniformly within the local frame there is no need to consider different types of edges. Therefore, the probability p_i that a failure message is passed from a variable node at position i is

$$p_i = \sum_r \lambda_r \bar{q}_i^{r-1} = \lambda(\bar{q}_i) \quad (49)$$

where

$$\bar{q}_i = \frac{1}{n} \sum_{j=i}^{i+n-1} q_j \quad (50)$$

is the average probability of the incoming edges to the variable node at position i . Similarly, it is possible to repeat the analysis in the previous Section for deriving that the probability that a check node at position i sends a failure message is

$$q_i = \sum_r \gamma_{i,r} \sum_{j \geq k} \binom{r-1}{j} \bar{p}_i^j (1-\bar{p}_i)^{r-1-j} = 1 - \sum_{j=0}^{k-1} \exp(-\eta_i) \frac{\eta_i^j}{j!} \quad (51)$$

where $\eta_i \triangleq \mu_i \bar{p}_i \Lambda'(1)/n$ and

$$\bar{p}_i = \begin{cases} \sum_{j=1}^i \frac{p_j}{i}, & 1 \leq i < n \\ \sum_{j=i-n+1}^i \frac{p_j}{n}, & i \geq n. \end{cases} \quad (52)$$

This completes the proof of the second statement in Theorem 2. The threshold λ_a^* is found by searching for the largest value of λ_a for which \bar{p}_i converges to 0 for all positions.

Define the auxiliary functions $g_k(x) = 1 - \exp(-\zeta x) \sum_{j=0}^{k-1} (\zeta x)^j / j!$ and $h_k(x) = \sum_{j=0}^{k-1} (\zeta x)^j / j! (\zeta x + k - j)$. Then, it is a straightforward yet long calculation to check that

$$U'_k(x) = \exp(-\zeta x) \left(h_k(x) - \frac{h'_k(x)}{\zeta} - \frac{\Lambda'(g_k(x))}{\Lambda'(1)} \zeta \frac{(\zeta x)^{k-1}}{(k-1)!} \right). \quad (53)$$

Using the identity

$$h'_k(x) = \zeta \sum_{j=0}^{k-1} \frac{(\zeta x)^{j-1}}{j!} + h_{k-1}(x), \quad (54)$$

plugging this into (53), and simplifying terms we get

$$U'_k(x) = \exp(-\zeta x) \zeta \frac{(\zeta x)^{k-1}}{(k-1)!} (x - \lambda(g_k(x))), \quad (55)$$

so the maximum of $U(x)$ is attained when the term between parentheses is zero. This proves the lemma.

REFERENCES

- [1] G. Aceto, V. Persico, A. Pescape, A survey on information and communication technologies for industry 4.0: State-of-the-art, taxonomies, perspectives, and challenges, *IEEE Communications Surveys & Tutorials* 21 (4) (2019) 3467–3501. doi:10.1109/comst.2019.2938259.
- [2] I. Leyva-Mayorga, C. Stefanovic, P. Popovski, V. Pla, J. Martinez-Bauset, Random access for machine-type communications (dec 2019). doi:10.1002/9781119471509.w5gref031.
- [3] Y. Liu, S. Zhang, X. Mu, Z. Ding, R. Schober, N. Al-Dhahir, E. Hossain, X. Shen, Evolution of NOMA toward next generation multiple access (NGMA) for 6G, *IEEE Journal on Selected Areas in Communications* 40 (4) (2022) 1037–1071. doi:10.1109/jsac.2022.3145234.
- [4] N. Abramson, The throughput of packet broadcasting channels, *IEEE Transactions on Communications* 25 (1) (1977) 117–128. doi:10.1109/tcom.1977.1093713.
- [5] E. Casini, R. D. Gaudenzi, O. Herrero, Contention resolution diversity slotted ALOHA (CRDSA): An enhanced random access scheme for satellite access packet networks, *IEEE Transactions on Wireless Communications* 6 (4) (2007) 1408–1419. doi:10.1109/twc.2007.348337.
- [6] G. Liva, Graph-based analysis and optimization of contention resolution diversity slotted ALOHA, *IEEE Transactions on Communications* 59 (2) (2011) 477–487. doi:10.1109/tcomm.2010.120710.100054.
- [7] O. del Rio Herrero, R. D. Gaudenzi, Generalized analytical framework for the performance assessment of slotted random access protocols, *IEEE Transactions on Wireless Communications* 13 (2) (2014) 809–821. doi:10.1109/twc.2013.121813.130435.
- [8] A. Meloni, M. Murrioni, C. Kissling, M. Berlioli, Sliding window-based contention resolution diversity slotted ALOHA, in: 2012 IEEE Global Communications Conference (GLOBECOM), IEEE, 2012. doi:10.1109/glocom.2012.6503624.
- [9] E. Sandgren, A. G. i Amat, F. Brannstrom, On frame asynchronous coded slotted ALOHA: Asymptotic, finite length, and delay analysis, *IEEE Transactions on Communications* 65 (2) (2017) 691–704. doi:10.1109/tcomm.2016.2633468.
- [10] Y. Polyanskiy, A perspective on massive random-access, in: 2017 IEEE International Symposium on Information Theory (ISIT), IEEE, 2017. doi:10.1109/isit.2017.8006984.
- [11] A. G. i Amat, G. Liva, Finite-length analysis of irregular repetition slotted ALOHA in the waterfall region, *IEEE Communications Letters* 22 (5) (2018) 886–889. doi:10.1109/lcomm.2018.2812845.
- [12] M. Ivanov, F. Brannstrom, A. G. i Amat, P. Popovski, Error floor analysis of coded slotted ALOHA over packet erasure channels, *IEEE Communications Letters* 19 (3) (2015) 419–422. doi:10.1109/lcomm.2014.2385073.
- [13] M. Ivanov, F. Brannstrom, A. G. i Amat, P. Popovski, Broadcast coded slotted ALOHA: A finite frame length analysis, *IEEE Transactions on Communications* 65 (2) (2017) 651–662. doi:10.1109/tcomm.2016.2625253.
- [14] T. Akyildiz, U. Demirhan, T. M. Duman, Energy harvesting irregular repetition ALOHA with replica concatenation, *IEEE Transactions on Wireless Communications* 20 (2) (2021) 955–968. doi:10.1109/twc.2020.3029387.
- [15] F. Clazzer, A. G. i Amat, Error floor analysis of irregular repetition ALOHA (Feb. 2022). arXiv:2202.07908.
- [16] B. Zhao, G. Ren, X. Dong, H. Zhang, Optimal irregular repetition slotted ALOHA under total transmit power constraint in IoT-oriented satellite networks, *IEEE Internet of Things Journal* 7 (10) (2020) 10465–10474. doi:10.1109/jiot.2020.2994296.
- [17] A. Mengali, R. D. Gaudenzi, P.-D. Arapoglou, Enhancing the physical layer of contention resolution diversity slotted ALOHA, *IEEE Transactions on Communications* (2017) 1–1. doi:10.1109/tcomm.2017.2696952.
- [18] F. Clazzer, C. Kissling, M. Marchese, Enhancing contention resolution ALOHA using combining techniques, *IEEE Transactions on Communications* 66 (6) (2018) 2576–2587. doi:10.1109/tcomm.2017.2759264.
- [19] S. Alvi, S. Durrani, X. Zhou, Enhancing CRDSA with transmit power diversity for machine-type communication, *IEEE Transactions on Vehicular Technology* 67 (8) (2018) 7790–7794. doi:10.1109/tvt.2018.2831926.
- [20] X. Shao, Z. Sun, M. Yang, S. Gu, Q. Guo, NOMA-based irregular repetition slotted ALOHA for satellite networks, *IEEE Communications Letters* 23 (4) (2019) 624–627. doi:10.1109/lcomm.2019.2900319.
- [21] M. Kazemi, T. M. Duman, M. Medard, Collision resolution for random access, *IEEE Transactions on Wireless Communications* 21 (5) (2022) 3464–3477. doi:10.1109/twc.2021.3122016.
- [22] C. R. Srivatsa, C. R. Murthy, User activity detection for irregular repetition slotted ALOHA based mMTC (Nov. 2021). arXiv:2111.06140.
- [23] M. Luby, M. Mitzenmacher, M. Shokrollahi, D. Spielman, Improved low-density parity-check codes using irregular graphs, *IEEE Transactions on Information Theory* 47 (2) (2001) 585–598. doi:10.1109/18.910576.
- [24] T. Richardson, M. Shokrollahi, R. Urbanke, Design of capacity-approaching irregular low-density parity-check codes, *IEEE Transactions on Information Theory* 47 (2) (2001) 619–637. doi:10.1109/18.910578.
- [25] C. Di, D. Proietti, I. Telatar, T. Richardson, R. Urbanke, Finite-length analysis of low-density parity-check codes on the binary erasure channel, *IEEE Transactions on Information Theory* 48 (6) (2002) 1570–1579. doi:10.1109/tit.2002.1003839.
- [26] E. Paolini, G. Liva, M. Chiani, Coded slotted ALOHA: A graph-based method for uncoordinated multiple access, *IEEE Transactions on Information Theory* 61 (12) (2015) 6815–6832. doi:10.1109/tit.2015.2492579.
- [27] C.-H. Yu, L. Huang, C.-S. Chang, D.-S. Lee, Poisson receivers: A probabilistic framework for analyzing coded random access, *IEEE/ACM Transactions on Networking* 29 (2) (2021) 862–875. doi:10.1109/tnet.2021.3050485.
- [28] C.-M. Chang, Y.-J. Lin, C.-S. Chang, D.-S. Lee, On the stability regions of coded poisson receivers with multiple classes of users and receivers (Jul. 2021). arXiv:2107.10696.
- [29] M. Ghanbarinejad, C. Schlegel, Irregular repetition slotted ALOHA with multiuser detection, in: 2013 10th Annual Conference on Wireless On-demand Network Systems and Services (WONS), IEEE, 2013. doi:10.1109/wons.2013.6578348.
- [30] I. Hmedoush, C. Adjih, P. Muhlethaler, V. Kumar, On the performance of irregular repetition slotted ALOHA with multiple packet reception, in: 2020 International Wireless Communications and Mobile Computing (IWCMC), IEEE, 2020. doi:10.1109/iwcmc48107.2020.9148173.
- [31] C. Dumas, L. Salaün, I. Hmedoush, C. Adjih, C. S. Chen, Design of coded slotted ALOHA with interference cancellation errors, *IEEE Transactions on Vehicular Technology* 70 (12) (2021) 12742–12757. doi:10.1109/tvt.2021.3120069.
- [32] A. Baiocchi, F. Ricciato, Analysis of pure and slotted ALOHA with multi-packet reception and variable packet size, *IEEE Communications Letters* 22 (7) (2018) 1482–1485. doi:10.1109/lcomm.2018.2834360.
- [33] C. Stefanovic, E. Paolini, G. Liva, Asymptotic performance of coded slotted ALOHA with multipacket reception, *IEEE Communications Letters* 22 (1) (2018) 105–108. doi:10.1109/lcomm.2017.2761768.
- [34] S. Ghez, S. Verdu, S. Schwartz, Stability properties of slotted ALOHA with multipacket reception capability, *IEEE Transactions on Automatic Control* 33 (7) (1988) 640–649. doi:10.1109/9.1272.
- [35] O. Y. Feng, R. Venkataraman, C. Rush, R. J. Samworth, A unifying tutorial on approximate message passing, *Foundations and Trends® in Machine Learning* 15 (4) (2022) 335–536. doi:10.1561/22000000092.